

COMPLETION OF STRUCTURALLY-INCOMPLETE MATRICES WITH REWEIGHTED LOW-RANK AND SPARSITY PRIORS

Jingyu Yang, Xuemeng Yang, Xinchen Ye

School of Electronic Information Engineering, Tianjin University
Building 26-D, No. 92, Weijin Road, Nankai District, Tianjin 300072, China

ABSTRACT

Most matrix completion methods impose a low-rank prior or its variants to well pose the problem. However, the rank minimization is problematic to handle matrices with structural missing. To remedy this, this paper introduces a new matrix completion method using double priors on the latent matrix, named Reweighted Low-rank and Sparsity Priors. In the proposed model, the matrix is regularized by a low-rank prior to exploit the inter-column (row) correlations, and its columns (rows) are regularized by a sparsity prior under a dictionary to exploit intra-column (row) correlations. Both the low-rank and sparse priors are reweighted on the fly to promote low-rankness and sparsity, respectively. Numerical algorithm to solve our model is derived via the alternating direction method under the augmented Lagrangian multiplier framework. Experimental results show that our model is quite effective in recovering matrices with highly-structural missing, complementing the classic matrix completion models that handle random missing only.

Index Terms— Matrix completion, low-rank approximation, sparse representation, inpainting

1. INTRODUCTION

In matrix completion, the latent matrix is assumed to have a low-rank structure so that the degrees of freedom can be determined by partial observed entries. Candès and Recht [1] proved that most low-rank matrices can be accurately completed from a small fraction of known entries under quite mild conditions, and the intractable rank minimization is relaxed into the nuclear norm minimization to have an efficient algorithm via convex programming. Low-rank matrix completion is also proven stable to small and bounded noise [2]. The recovery guarantees are improved for the case of bounded rank in [3]. The basic matrix completion model has many extensions with more powerful modelings, e.g., RPCA [4] and L-RR [5].

This work was supported by National Natural Science Foundation of China (NSFC) under Grant 61372084 and 61520106002, and by the Reserved Peiyang Scholar Program of Tianjin University, Tianjin, China.

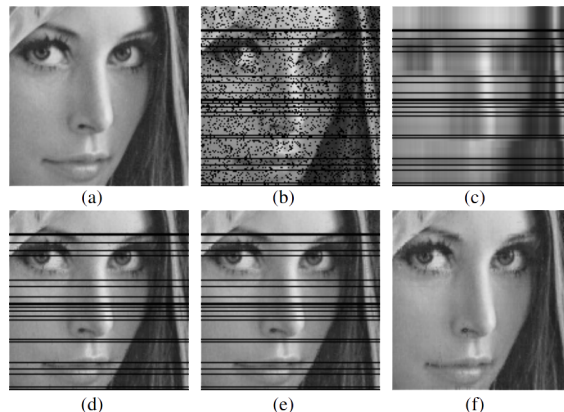


Fig. 1. Matrix completion examples. (a) original *Lena* patch; (b) observation patch with 30% missing entries shown in black; (c) IALM [6] (13.47/0.27); (d) SVT [7] (13.93/0.41); (e) FaLRTC [8] (14.17/0.42), and (f) Ours (35.39/0.96). The performances are measured by (PSNR/SSIM).

Many algorithms have been proposed for solving low-rank matrix approximation, e.g., the singular value thresholding (SVT) [7], augmented lagrangian multiplier method (ALM) [6], and accelerated proximate gradient algorithm (APG) [9]. The nuclear norm is proposed to be iteratively reweighted to promote low-rankness [10], inspired by the reweighted ℓ_1 norm minimization in sparse representation [11]. Being quite versatile and equipping with efficient numerical algorithms, low-rank matrix approximation models achieve prominent performance in many applications such as face recognition [12], background modeling [13], and 3D reconstruction [14]. Previous models [1, 2] generally assume that the locations of missing entries are random, and each row or column should have some observed entries. However, the assumption can be violated in practical applications. For example, in background modeling, missing locations are determined by the moving trajectories of foreground objects. Another example in Fig. 1, We crop the portion from the *Lena* image, some pixels are removed to simulate both random and entire-row missing. Three previous method-

s, SVT [7], ALM [6], FaLRTC [8] are able to reconstruct randomly-missing entries, but cannot handle the entire-row missing. Liu et al. [5] propose Low-Rank Representation (LRR), which seeks the lowest rank representation among all the candidates that can represent the data. This can cluster the data into their respective subspaces. In [15], the power-law distribution sampled matrix completion problem has been addressed instead of matrix sampled randomly. In [16], the situation that large portions of columns are corrupted, is considered. However, these methods fail to reconstruct the entire-row missing matrix. Therefore, the recovery of structurally-incomplete matrices is still a challenging task.

In this paper, we propose to use reweighted low-rank and sparsity priors (ReLaSP) to recover matrices with structural missing. Our model is based on the observation that rows/columns in interested matrices are signals of strong intra-correlations, e.g., image lines/blocks, temperature field at a particular time instant. In our ReLaSP model, the matrix is regularized by a low-rank prior to exploit inter-column/row correlations and simultaneously by a sparsity priors on its columns to exploit intra-column correlations¹. An alternating direction method under augmented Lagrangian multiplier (ALM-ADM) framework is derived to solve the ReLaSP model. Both the low-rank and sparsity priors are reweighted at each iteration to promote low-rankness and sparseness. The effectiveness of our model is demonstrated by experiments on both synthetic data and image restoration task.

2. PROPOSED RELASP MODEL

2.1. ReLaSP Model

Let D be an incomplete version of matrix A . The observed matrix D contains both structural and random missing, and Ω denotes the index set of known entries. To remedy the deficiency of the low-rank prior on structural missing, we further assume that each column of A has sparse presentation under dictionary Φ , and B is the corresponding coefficient matrix. Recent work [10, 11] show that reweighing of the priors significantly promote the sparsity and low-rankness. Hence, we propose the following matrix completion model with reweighted low-rank and sparsity priors (ReLaSP):

$$\begin{aligned} & \min \operatorname{tr}(W_a \circ \Sigma) + \gamma \|W_b \circ B\|_1 \\ \text{s.t. } & A = \Phi B, \\ & \mathcal{P}_\Omega(A) = \mathcal{P}_\Omega(D), \end{aligned} \quad (1)$$

where $\operatorname{tr}(\cdot)$ denotes the trace of a matrix, \circ stands for the element-wise product of two matrices (also known as Hadamard product), and $\Sigma := \operatorname{diag}([\sigma_1, \sigma_2, \dots, \sigma_n])$ is a diagonal matrix that contains singular values of A with a

¹To maintain a concise presentation, we apply the sparsity prior to columns against entire-row missing. The sparsity prior can also be applied to columns or both rows and columns to handle column missing or both row-column missing, respectively.

non-increasing order from σ_1 to σ_n , $\mathcal{P}_\Omega(\cdot)$ denotes the projection operator onto Ω . W_a and W_b are weighting matrices for weighted nuclear norm $\operatorname{tr}(W_a \circ \Sigma)$ and weighted ℓ_1 norm $\|W_b \circ B\|_1$, respectively.

For convenient manipulation, we introduce an auxiliary error matrix, and transfer the matrix completion problem to a special case of matrix recovery problem, i.e., setting the missing entries as zeros. The ReLaSP model can be reformulated as follows

$$\begin{aligned} & \min \operatorname{tr}(W_a \circ \Sigma) + \gamma \|W_b \circ B\|_1 \\ \text{s.t. } & A = \Phi B, \\ & A + E = D, \mathcal{P}_\Omega(E) = 0, \end{aligned} \quad (2)$$

where E compensates for the missing entries.

2.2. Algorithm for ReLaSP Model

In sparse representation, we minimize the ℓ_1 norm instead of minimizing the non-smooth and non-convex ℓ_0 norm. The reweighting scheme aims to rectify the difference between the smooth surrogate and the original function [11]. To this end, small coefficients are assigned with large weights to encourage smaller values towards zeros in the next round of optimization, while large coefficients are assigned with small weights conversely. Similarly, the reweighting on the nuclear norm is also to further approximate the rank function, and the weights on singular values are assigned in a similar way [10]. The weighting matrix W_a and W_b are initialized at equal weights, and then updated according to the estimated singular values Σ^l and coefficient matrix B^l , use the inverse proportion rule [11]. We present a brief iterative algorithm for the reweighting framework in Algorithm 1.

Given the weighting matrix, the proposed ReLaSP model (1) is a minimization function with equality constraints. We choose the augmented Lagrangian method (ALM) [17] to handle the equality constraints under an iterative framework. As the ReLaSP model has multiple sets of variables. We use the alternative direction method (ADM) [18] to alternatively optimize one with others fixed at each ALM iteration. We derive the ALM-ADM algorithm for the ReLaSP model (1) in Algorithm 2. To have a light exposition, the superscript denoting iteration index in weighting matrices W_a^l and W_b^l are dropped.

Algorithm 1 (Reweighting framework)

- 1: **Input:** Set iteration counter $l = 0$, $W_a^0(i, i) = 1$, $W_b^0(i, j) = 1$, $\varepsilon > 0$;
 - 2: **while** not converged **do**
 - 3: Solve A^{l+1} and B^{l+1} via Algorithm (2) given W_a^l and W_b^l ;
 - 4: $W_a^{l+1}(i, i) = \frac{1}{\sigma_i^l + \varepsilon}$, $W_b^{l+1}(i, j) = \frac{1}{|B^l(i, j)| + \varepsilon}$;
 - 5: **end while**
 - 6: **Output:** A
-

Algorithm 2 (ALM-ADM algorithm for Model (2))

- 1: **Input:** observation matrix $D \in R^{m \times n}$, dictionary $\Phi \in R^{m \times p}$, $A^1 = E^1 = Y_1^1 = Y_2^1 = \mathbf{0} \in R^{m \times n}$, $B^1 = \mathbf{0} \in R^{p \times n}$, $k = 1$, $\mu_1^1 = \mu_2^1 > 0$, $\rho_1 = \rho_2 > 1$
- 2: **while** not converged **do**
- 3: $t_1 = j = 1, B_1^k = B^k, Z_1 = B^k$
- 4: //Line 4-11 solve subproblem-B
- 5: **while** not converged **do**
- 6: $U_{j+1} = Z_j - \frac{\mu_1^k}{L_f} \Phi^\top \left(\Phi Z_t - \frac{1}{\mu_1^k} Y_1^k - A^k \right)$
- 7: $B_{j+1}^k = \text{soft} \left(U_{j+1}, \frac{\gamma}{L_f} W_b \right)$
- 8: $t_{j+1} = \frac{1 + \sqrt{4t_j^2 + 1}}{2}$
- 9: $Z_{j+1} = B_{j+1}^k + \frac{t_j - 1}{t_{j+1}} (B_{j+1}^k - B_j^k)$
- 10: **end while**
- 11: $B^{k+1} = B_{j+1}^k$
- 12: //Line 12-14 solve subproblem-A
- 13: $(U^k, \Sigma^k, V^k) = \text{svd}(W^k)$

$$W^k = \frac{(Y_2^k - Y_1^k + \mu_1^k \Phi B^{k+1} - \mu_2^k E^k + \mu_2^k D)}{\mu_1^k + \mu_2^k}$$

- 14: $A^{k+1} = U^k \text{soft} \left(\Sigma^k, \frac{w_a}{\mu_1^k + \mu_2^k} \right) V^{k\top}$
 - 15: //Line 16 solve subproblem-E
 - 16: $E^{k+1} = \mathcal{P}_\Omega(0) + \mathcal{P}_\Omega \left(\frac{Y_2}{\mu_2} + D - A \right)$
 - 17: $Y_1^{k+1} = Y_1^k + \mu_1^k (A^{k+1} - \Phi B^{k+1})$
 - 18: $Y_2^{k+1} = Y_2^k + \mu_2^k (D - A^{k+1} - E^{k+1})$
 - 19: $\mu_1^{k+1} = \rho_1 \mu_1^k, \mu_2^{k+1} = \rho_2 \mu_2^k$
 - 20: **end while**
 - 21: **Output:** $A^* = A^{k+1}, \Sigma^* = \Sigma^{k+1}$
 $B^* = B^{k+1}, E^* = E^{k+1}$
-

3. EXPERIMENTAL RESULTS

Our proposed algorithm is evaluated both on synthetic data and real images. For all the experiments, parameters are set as follows: $\varepsilon = 0.001$, $\rho_1 = \rho_2 = 1.1$, $\gamma = 0.1$, $\mu_1 = \mu_2 = 0.5/\max(\sigma(D))$, where $\sigma(D)$ denotes the singular values of D . We use relative error (RE) to measure the results: $RE = \|A^* - A\|_F / \|A\|_F$, where A is the groundtruth and A^* is the reconstruction data. The performances in image restoration are measured by the peak signal-to-noise ratio (PSNR) and structural similarity (SSIM) [19].

3.1. Results on Synthetic Data

In the synthetic experiment, we construct the low-rank matrix based on a randomly generated dictionary. With different matrix size (n), matrix rank ($rank$), missing rate (Mr), entire row missing rate (Lr), and coefficient sparseness (spa), we conduct the synthetic experiments under different situation. Our method is compared with two state-of-the-art algorithms, i.e., SVT [7] and IALM [6]. Numerical results are shown in

Table 1. RelaSP-0 and RelaSP-2 represent our method without reweighting scheme and with two reweighting iterations, respectively. We observe that our method achieves the best result under all the configurations. SVT and IALM can reconstruct matrices with random missing at low-to-middle missing rates, but fail at high missing rates. However, both SVT and IALM fail for all the cases with entire-row missing. RelaSP-2 has better results than RelaSP-0 for most cases, which verifies the effectiveness of reweighting in sparsity and low-rankness.

3.2. Results on Exact Recoverability

We present a visible result to demonstrate exact recoverability of SVT [7] and our model. Test data is generated in the same way in section 3.1. Results can be seen in Fig. 2 for rank varies from 1 to 50 and missing rate from 1% to 50%. For each pair of ($rank, Mr$), we repeat experiment 7 times and claim for recovery successfully when $RE \leq 1E - 4$. The results demonstrate the ambiguity and limitation of rank minimization in regularizing entire-row missing entities.

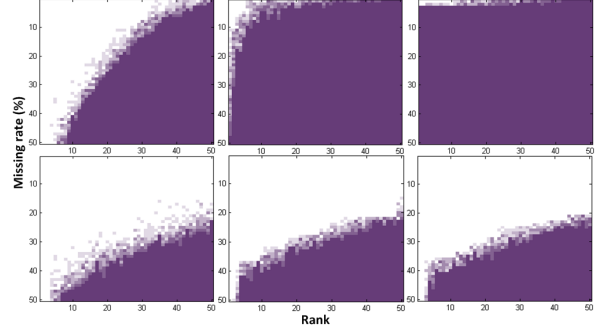


Fig. 2. Recoverability results of SVT [7] (top row) and ReLaSP-2 (bottom row). Left column: random missing; middle column: structural but no entire-row missing; right column: structural and entire-row missing ($Lr = 0.2$). The color varies from white to purple representing recoverability varies from 100% to 0%.

3.3. Results on Image Restoration

In the experiment, a fixed global dictionary of size 30×300 is obtained by online dictionary learning method [22] on Kodak image set [23]. The training data contains 500,000 image segments of the size 30×1 which are selected randomly. We divide the input corrupted image into 30×512 patches (512 = the width of the image.) in a sliding way, and apply our algorithm on each patch. Our algorithm is compared with three algorithms, i.e., Fast Low Rank Tensor Completion (FaLRTC) [8], deterministic annealing method (DA-based) [20] and OMP [21]. The results of three methods are generated by the provided codes, and the optimal parameters are tuned for fair comparison. Table 2 shows results in term

Table 1. Relative error comparison for matrix reconstruction on synthetic data in different configurations.

Data	Mr	25%			50%			75%		
	Lr	0%	30%	60%	0%	30%	60%	0%	30%	60%
n=300 rank=15 spa=5%	SVT [7]	1.21E-04	0.2814	0.3858	1.89E-04	0.3908	0.5517	0.1652	0.4891	0.6724
	IALM [6]	1.12E-04	0.2814	0.3858	1.64E-04	0.3908	0.5517	0.0012	0.4710	0.6724
	MC-ReLaSP-0	4.42E-05	6.92E-05	8.78E-05	7.39E-05	9.09E-05	1.11E-04	1.90E-04	2.63E-04	2.23E-04
	MC-ReLaSP-2	5.07E-05	5.36E-05	5.51E-05	7.55E-05	8.37E-05	8.85E-05	9.34E-05	1.02E-04	1.09E-04
n=400 rank=20 spa=7%	SVT [7]	1.16E-04	0.2722	0.3875	1.50E-04	0.3843	0.5498	0.1305	0.6035	0.6652
	IALM [6]	9.64E-05	0.2722	0.3875	1.48E-04	0.3843	0.5498	4.49E-04	0.4788	0.6652
	MC-ReLaSP-0	4.71E-05	6.20E-05	9.09E-05	6.77E-05	8.58E-05	1.12E-04	1.56E-04	1.62E-04	2.05E-04
	MC-ReLaSP-2	5.17E-05	5.41E-05	5.95E-05	7.24E-05	8.10E-05	9.15E-05	9.46E-05	9.74E-05	1.05E-04
n=500 rank=25 spa=10%	SVT [7]	1.10E-04	0.2720	0.3883	1.52E-04	0.3888	0.5493	0.1379	0.4839	0.6703
	IALM [6]	1.02E-04	0.2720	0.3883	1.34E-04	0.3888	0.5493	2.78E-04	0.4801	0.6703
	MC-ReLaSP-0	4.70E-05	5.73E-05	9.21E-05	6.70E-05	8.97E-05	1.13E-04	1.33E-04	1.45E-04	2.15E-04
	MC-ReLaSP-2	5.10E-05	5.59E-05	6.15E-05	7.35E-05	8.42E-05	1.01E-04	9.65E-05	9.63E-05	1.18E-04

Table 2. Quantitative Results (PSNR(dB)/SSIM) for images restoration at different missing rates

Images	Mr	5%	10%	20%	30%	50%
Lena	FaLRTC [8]	24.99/0.9048	22.51/0.8053	19.29/0.6404	17.24/0.5468	15.00/0.4106
	DA-based [20]	39.35/0.9881	39.60/0.9907	31.45/0.9486	29.25/0.9281	27.57/0.8985
	OMP [21]	36.96/0.9745	33.61/0.9526	29.86/0.8985	27.39/0.8588	23.37/0.7484
	ReLaSP	46.40/0.9987	42.09/0.9968	37.98/0.9913	35.05/0.9838	31.20/0.9589
Gulls	FaLRTC [8]	30.45/0.9440	26.23/0.8750	22.66/0.7526	20.67/0.6371	18.39/0.5034
	DA-based [20]	37.15/0.9933	34.44/0.9919	28.88/0.9737	28.05/0.9659	24.60/0.9256
	OMP [21]	36.89/0.9869	34.66/0.9766	30.77/0.9467	28.74/0.9118	25.23/0.8416
	ReLaSP	43.82/0.9985	41.72/0.9970	37.08/0.9918	34.69/0.9842	30.22/0.9599
Hill	FaLRTC [8]	27.51/0.9145	21.50/0.8330	19.26/0.7233	17.29/0.6043	15.34/0.4513
	DA-based [20]	35.87/0.9832	30.18/0.9470	26.77/0.9318	25.13/0.9104	23.68/0.8588
	OMP [21]	35.94/0.9772	33.01/0.9544	29.57/0.9142	27.76/0.8677	23.69/0.7617
	ReLaSP	43.09/0.9962	39.44/0.9915	35.90/0.9843	34.04/0.9711	30.02/0.9224
Bridge	FaLRTC [8]	27.77/0.9162	26.22/0.8567	23.23/0.7336	20.39/0.5996	18.83/0.4817
	DA-based [20]	35.56/0.9881	32.98/0.9813	31.66/0.9754	28.91/0.9507	29.87/0.9299
	OMP [21]	38.94/0.9871	36.57/0.9739	32.83/0.9464	30.27/0.9118	27.04/0.8467
	ReLaSP	46.92/0.9988	44.38/0.9973	39.37/0.9921	36.83/0.9842	32.91/0.9606

of PSNR/SSIM. Our method achieves the best performance for all cases. We observe that the PSNR/SSIM value of FaLRTC is relatively lower because of the failure of completing entire-row missing. The DA-based method has comparable PSNR/SSIM values with us at low missing rates, but has lower values at high missing rate. The OMP method has passable PSNR but the SSIM is lower because of blur. Visual quality comparisons on *Bridge* is shown in Fig. 3. The DA-based method and OMP can deal with the entire-row missing, but their results are subject to many line-like artifacts, such as the surface of the road. The combination of low-rank prior and sparse prior in our model plays a crucial role in dealing with random missing and structural missing.

4. CONCLUSION

This paper introduces the Reweighted Low-rank and Sparsity Priors (ReLaSP). Based on this, a new matrix completion method is proposed. Both the low-rank and sparse priors are reweighted on the fly to promote low-rankness and sparsity, respectively. The reweighted ALM-ADM framework is used to solve our ReLaSP model. Experimental results show the superior performance of our ReLaSP model.

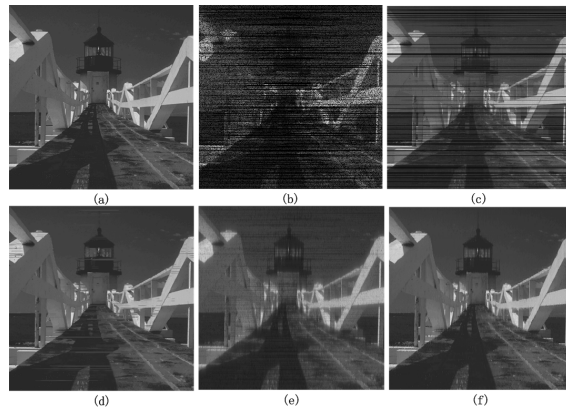


Fig. 3. Restoration result of *Bridge* with 50% pixels missing. (a) Ground; (b) Damaged; (c) FaLRTC [8] (18.83/0.4817); (d) DA-based [20] (29.87/0.9299); (e) OMP [21] (27.04/0.8467), and (f) Ours (32.91/0.9606).

5. REFERENCES

- [1] E. J. Candès and B. Recht, “Exact matrix completion via convex optimization,” *Foundations of Computational mathematics*, vol. 9, no. 6, pp. 717–772, 2009.
- [2] E. J. Candès and Y. Plan, “Matrix completion with noise,” *Proceedings of the IEEE*, vol. 98, no. 6, pp. 925–936, 2010.
- [3] R. H. Keshavan, A. Montanari, and S. Oh, “Matrix completion from a few entries,” *IEEE Trans. Information Theory*, vol. 56, no. 6, pp. 2980–2998, 2010.
- [4] E. J. Candès, X. Li, Y. Ma, and J. Wright, “Robust principal component analysis?,” *Journal of the ACM (JACM)*, vol. 58, no. 3, pp. 11, 2011.
- [5] G. Liu, Z. Lin, S. Yan, J. Sun, Y. Yu, and Y. Ma, “Robust recovery of subspace structures by low-rank representation,” *IEEE Trans. Pattern Analysis and Machine Intelligence*, vol. 35, no. 1, pp. 171–184, 2013.
- [6] Z. Lin, Mi. Chen, and Y. Ma, “The augmented lagrange multiplier method for exact recovery of corrupted low-rank matrices,” *arXiv preprint arXiv:1009.5055*, 2010.
- [7] J.-F. Cai, E. J. Candès, and Z. Shen, “A singular value thresholding algorithm for matrix completion,” *SIAM Journal on Optimization*, vol. 20, no. 4, pp. 1956–1982, 2010.
- [8] J. Liu, P. Musialski, P. Wonka, and J. Ye, “Tensor completion for estimating missing values in visual data,” *IEEE Trans. Pattern Analysis and Machine Intelligence*, vol. 35, no. 1, pp. 208–220, 2013.
- [9] K.-C. Toh and S. Yun, “An accelerated proximal gradient algorithm for nuclear norm regularized linear least squares problems,” *Pacific Journal of Optimization*, vol. 6, no. 615–640, pp. 15, 2010.
- [10] Y. Peng, J. Suo, Q. Dai, and W. Xu, “Reweighted low-rank matrix recovery and its application in image restoration,” *IEEE Trans. Cybernetics*, vol. 44, no. 12, pp. 2418–2430, 2014.
- [11] E. J. Candès, M. B. Wakin, and S. P. Boyd, “Enhancing sparsity by reweighted ℓ_1 minimization,” *Journal of Fourier Analysis and Applications*, vol. 14, no. 5–6, pp. 877–905, 2008.
- [12] K. Jia, T.-H. Chan, and Y. Ma, “Robust and practical face recognition via structured sparsity,” in *Eur. Conf. Computer Vision*, pp. 331–344. Springer, 2012.
- [13] X. Ye, J. Yang, X. Sun, K. Li, C. Hou, and Y. Wang, “Foreground-background separation from video clips via motion-assisted matrix restoration,” *IEEE Trans. Circuits and Systems for Video Technology*, vol. PP, no. 99, pp. 1721–1734, 2015.
- [14] H. Mobahi, Z. Zhou, A. Y. Yang, and Y. Ma, “Holistic 3D reconstruction of urban structures from low-rank textures,” in *Int. Conf. Computer Vision Workshops. IEEE*, 2011, pp. 593–600.
- [15] R. Meka, P. Jain, and I. S. Dhillon, “Matrix completion from power-law distributed samples,” in *Advances in Neural Information Processing Systems*, 2009, pp. 1258–1266.
- [16] Y. Chen, H. Xu, C. Caramanis, and S. Sanghavi, “Robust matrix completion and corrupted columns,” in *Int. Conf. Machine Learning*, 2011.
- [17] D. P. Bertsekas, “Constrained optimization and lagrange multiplier methods,” *Computer Science and Applied Mathematics, Boston: Academic Press*, vol. 1, 1982.
- [18] S. Boyd, N. Parikh, E. Chu, B. Peleato, and J. Eckstein, “Distributed optimization and statistical learning via the alternating direction method of multipliers,” *Foundations and Trends in Machine Learning*, vol. 3, no. 1, pp. 1–122, 2011.
- [19] Z. Wang, A. C. Bovik, H. R. Sheikh, and E. P. Simoncelli, “Image quality assessment: from error visibility to structural similarity,” *IEEE Trans. Image Processing*, vol. 13, no. 4, pp. 600–612, 2004.
- [20] X. Li, “Image recovery via hybrid sparse representations: A deterministic annealing approach,” *IEEE Journal of Selected Topics in Signal Processing*, vol. 5, no. 5, pp. 953–962, 2011.
- [21] <http://spams.devel.gforge.inria.fr/>, “Sparse modeling software,” .
- [22] J. Mairal, F. Bach, J. Ponce, and G. Sapiro, “Online dictionary learning for sparse coding,” in *Int. Conf. Machine Learning. ACM*, 2009, pp. 689–696.
- [23] <http://r0k.us/graphics/kodak/>, “Kodak lossless true color image suite,” .